RSC Advances

ROYAL SOCIETY OF CHEMISTRY

www.rsc.org/advances

Journal Name

RSCPublishing

ARTICLE

A novel sp^3Al-based porous single-ion polymer electrolyte for lithium ion batteries

Cite this: DOI: 10.1039/x0xx00000x

Guodong Xu,[a] Rupesh Rohan,[a] Jing Li[a,b] and Hansong Cheng*[a,b]

Received 00th January 2012,
Accepted 00th January 2012

DOI: 10.1039/x0xx00000x

www.rsc.org/

We report synthesis of an Al-based porous gel single-ion polymer electrolyte, lithium poly (glutaric acid aluminate) (LiPGAA), using glutaric acid and lithium tetramethanolatoaluminate as the precursors. The three-dimensional network compound provides short lithium-ion transport pathways and allows organic solvents to be accommodated in the composite for rapid ion transport. The tetraalkoxyaluminate units in the material enable Li-ions to be weakly associated with the polymeric framework, leading to a high ionic conductivity of 1.47 x 10^{-4} S cm^{-1} at room temperature and a high Li-ion transference number of 0.8. A membrane of the polymer was prepared via solution cast with PVDF-HFP (poly(vinylidene-fluoride-co-hexafluoropropene) followed by soaking in a solution of ethylene carbonate (EC) and propylene carbonate (PC) (v/v, 1:1). A Li-ion battery assembled with the composite membrane displays remarkable cyclability with nearly 100% coulombic efficiency over a wide temperature range.

Introduction,

Technology development of battery devices with high energy density and long cycle life is important to meet the ever-increasing energy storage challenge for various technological applications.[1-4] As one of the essential components in a lithium ion battery, an electrolyte plays a key role in enabling high energy density in the device.[5, 6] For the next generation Li-ion batteries, which utilize high energy density materials in the electrodes, an electrolyte with a high voltage tolerance is required in order to take full advantage of the amount of available power offered by the electrodes. In addition, the electrolyte must be able to overcome the chronic problem of anion concentration polarization during charge and discharge process, which is often observed with the typical dual-ion conductor electrolytes including liquid electrolytes and inorganic lithium salt based polymer electrolytes. The concentration polarization leads to an increased resistance and ultimate depletion of the electrolyte.[7-10] Recently, many single-ion polymer electrolytes (SIPEs) have been developed to minimize the cell polarization for high power applications.[11-17] Unfortunately, the majority of these materials display relatively low ionic conductivity on the order of 10^{-5} S cm^{-1} at room temperature, which allows batteries to perform only at elevated temperatures. In the last few years, many researchers have reported SIPEs with a variety of polymeric structural designs. These electrolyte materials have been shown to exhibit high thermostability, high ionic conductivity, high Li-ion transference numbers, broad electrochemical windows and remarkable battery performance.[18-24]

Lithium tetraalkoxyaluminates have been considered as good candidates for electrolytes of Li-ion batteries because the weak coordination between the lithium ions and the counter-anions, promoting the solvation of Li-ions in aprotic organic solvents.[25, 26] The first study on tetraalkoxyaluminate unit was to synthesize trialcohol substituted lithium aluminumhydride, particularly lithium tri-t-butoxyaluminatehydride, which is stable up to 300 ^oC.[27] Subsequently, a few tetraalkoxyaluminate based compounds have been synthesized, among which lithium

tetra (1, 1, 1, 3, 3, 3-hexafluoro-2-propyl) aluminate (LiAl(HFIP)) and lithium tetra (1, 1, 1, 3, 3, 3-hexafluoro-2-phenylpropyl) aluminate (LiAl(HFPP)) are the most prominent representatives. These materials exhibit a broad electrochemical window up to 5V, high ionic conductivity around 10^{-3} S cm^{-1} and moderate thermal stability up to 100 ^{o}C, resulting from the large anionic size and electron delocalization induced by the four electron-withdrawing groups attached to the central aluminium atom.[28-30] To circumvent the problems inherently associated with liquid dual-ion electrolytes, a number of solid single-ion electrolytes based on tetraalkoxyaluminate and polyfluoroalkoxyl groups, have also been synthesized.[31-33] These materials were made from $LiAlH_4$ (or partially substituted $LiAlH_4$) and diols with long aliphatic chains, particularly low molecular weight poly (ethyl glycol)s. The polymers were amorphous with a low lithium content. Despite offering a high Li-ion transference number and a low glass transition temperature, these solid polymers failed to perform as electrolytes when assembled in batteries, largely due to the low ionic conductivity on the order of 10^{-5} S cm^{-1} at room temperature.

The utilization of a plasticizer (e. g. EC and PC) may provide an effective way to enhance the flexibility of polymer chains and thus reduce ion pairing and improve electrode/electrolyte interfacial contact, which ultimately enhances lithium ionic conductivity and battery performance. In this paper, we present a protocol to synthesize a novel porous gel single-ion polymer electrolyte, lithium poly(glutaric acid aluminate) (LiPGAA), as described in Scheme 1. The use of a short ligand offers two advantages. One is to increase the polymer crystallinity, resulting in a porous structure, which facilitates accommodation of organic solvent molecules. Another is to increase the lithium content with a higher Al weight ratio. The SIPE membrane was prepared using a solution cast method with PVDF-HFP as the binder. The structure, surface morphology, thermal stability and electrochemical performance of the as-synthesized compound and its membrane were systematically investigated.

Results and discussion

The formation of LiPGAA was confirmed by ^{27}Al NMR (in reference to 1M $Al(NO_3)_3$) with a chemical shift at -5.72 ppm, compared with the signal of the starting material $LiAl(OCH_3)_4$, which is at 69.57 ppm. The ^{13}C MAS NMR (in reference to DMSO) indicates three different carbons with chemical shifts at 180.31 ppm, 36.07 ppm, and 21.14 ppm, respectively, which correlates well with the glutaric acid backbones. The coherence between the calculated and the found elemental analysis values also validates the successful synthesis of LiPGAA.

The thermogravimetric analysis of LiPGAA under nitrogen is shown in Figure 1. The TGA curve begins with an approximately 5% weight loss before 150 ^{o}C, which is attributed to the absorbed moisture or the trapped solvent molecules. Subsequently, no weight loss is observed until the temperature reaches roughly 350 ^{o}C at which the compound undergoes obvious decomposition. The residue weight left is approximately 30% corresponding to aluminum oxide and lithium oxide, which correlates well with the elemental analysis results. The result suggests that this compound is highly thermally stable.

The surface morphology of the polymer was examined with P-XRD and FE-SEM, respectively (Figure 2). The XRD patterns of LiPGAA (left) display sharp diffraction peaks, suggesting good crystallinity as expected. The FE-SEM images (right) show that the powder exhibits small flake shape structures stacking together, indicating that some planar structures may also be formed, similar to the results reported in a previous study.[34, 35]

The surface porosity was characterized by nitrogen isotherm at 77K at 1 bar (Figure 3). The isotherm displays a steep gas uptake at low pressure and capillary condensation at high pressure. The BET surface area was calculated to be 93.9 m^2/g, while the Langmuir surface area was 149.7 m^2/g. The pore size distribution gives a wide range of mesopores, centered at approximately 15 nm.

To calculate the ionic conductivity of the electrolyte membrane, the following equation was used: $\sigma = l/Ra$, where σ is the ionic conductivity, l denotes the thickness of the electrolyte membrane, R stands for the bulk resistance (R1 is shown in the equivalent circuit in Figure 4) and a represents the surface area. The EIS response of the membrane at room temperature with the circuit diagram used for fitting is shown in Figure 4. The ionic conductivity of the membrane was calculated to be 1.47 x 10^{-4} S cm^{-1} at room temperature, which is comparable to the values of most reported gel SIPEs.[36, 37] The as-synthesized polymer contains a high proportion of aluminium centers, which gives rise to high rigidity of the framework. As a consequence, the glass transition temperature

of the polymer is raised substantially (over 300 ^{o}C). The high rigidity of the polymer also results in lower ionic conductivity because the contribution to ion transport from the segmental motion is reduced. Hence, the high σ value is mainly attributed to the porous structure, which enables solvent molecules to be accommodated and thus promotes solvation of Li-ions in the polymer matrix.[28]

The temperature dependency of the ionic conductivity of the electrolyte membrane on the inverse of absolute temperature in the form of an Arrhenius plot is depicted in Figure 5. The measurements were conducted between 80 ^{o}C and 25 ^{o}C downwards. An important observation is that the plot shows a small curvature,[15, 38] unlike the behaviour of liquid electrolytes and small lithium-salt based dual-ion polymer electrolytes. This small curvature is commonly observed in other SIPEs, which reflects the mechanical coupling between ion transport and polymer host mobility.[35, 37] The highest ionic conductivity at 80 ^{o}C is 5.32 x 10^{-4} S cm^{-1}.

The electrochemical stability of the composite membrane was measured via linear sweep voltammetry (LSV) using a lithium foil as the counter and reference electrode. The measurement was carried out between 2.5 V and 6.5V (versus Li^{+}/Li) (Figure 6). The SIPE was found to be stable up to 4.2 V. To further characterize the membrane, cyclic voltammetry (CV) with and without EC and PC was conducted (Figure 7). The electrolyte CV with EC and PC is consistent with the LSV result, indicating a broad electrochemical window. However, there is no current signal for the CV of the composite membrane without EC and PC, suggesting an open circuit due to lack of an organic solvent to solvate the Li^{+} ions. Consequently, it is difficult for the Li^{+} ions to transport from the membrane to the Li foil.

The Li-ion transference number ($t_{Li^{+}}$) was measured by sandwiching the prepared membrane between two lithium electrodes.[39] The value was derived using the equation proposed by Evans and co-workers (Table 1).[40] The $t_{Li^{+}}$ value was found to be 0.80 at room temperature, modestly smaller than unity but substantially higher than the values for small inorganic lithium salt based electrolytes. The result suggests that the electrolyte membrane behaves indeed as a single-ion conductor.

To further analyze the electrochemical performance of LiPGAA, a battery with $LiFePO_4$ as the cathode and a Li foil as the anode was assembled using the membrane as the electrolyte. Cycle tests were conducted at 25 ^{o}C, 60 ^{o}C and 80 ^{o}C, respectively, for various C-rates as shown in Figure 8. The battery displays significant performance at room temperature, while most of the reported SIPE-based Li-ion batteries are operative only at elevated temperatures.[19] The discharge capacity at 0.1 C increased in the first few cycles at room temperature, probably due to the steady formation of ordered channels for Li-ion conduction. Unfortunately, the battery failed to perform at higher C rates at room temperature, which is attributed to the large interfacial resistance as shown in Figure 4. It is likely that the high interfacial resistance arises from the high rigidity of the polymer, leading to poor compatibility between the electrolyte and the electrodes. With increasing temperature, battery performance was enhanced with better discharge capacity even at higher C-rates. The coulombic efficiency of the battery became nearly 100% from room temperature to 80 ^{o}C. Figure 9 depicts the discharge profiles of the Li/LiPGAA/PVDF-HFP/$LiFePO_4$ battery at 80 ^{o}C at different power rates. The discharge profiles were measured to be 147 mAh g^{-1} at 0.1 C, 140 mAh g^{-1} at 0.2 C and 120 mAh g^{-1} at 0.5 C. Obviously, improving the compatibility between the membrane and the electrodes is essential for enhancement of the battery performance.

Overall, LiPGAA exhibits high thermostability and ionic conductivity comparable to the properties of other SIPEs. The lithium ion transference number of the material is somewhat inferior to the values of other SIPE materials, chiefly resulting from the low solubility of three dimensional framework in common organic solvents, hindering the formation of a high molecular weight polymer in the synthesis. Detail comparison of the properties is shown in Table S1 (supporting information).

Conclusions

We have demonstrated an approach to synthesize an aluminium based porous single-ion polymer electrolyte, LiPGAA. The method to prepare tetramethanolatoaluminate can be employed to synthesize a family of this type of compounds. LiPGAA is the first tetraalkoxyaluminate-based polymeric electrolyte membrane ever made with good battery performance to our knowledge. The structure and properties of LiPGAA and the composite membrane have been well characterized via elemental analysis, nuclear magnetic resonance,

thermogravimetric analysis, nitrogen isotherm and electrochemical impedance spectroscopy. The mesoporous polymer electrolyte displays excellent thermal stability up to 350 ^{o}C and high ionic conductivity of 1.47 x 10^{-4} S cm^{-1} at room temperature. The measured Li-ion transference number of 0.80 is substantially higher than the values of liquid electrolytes and inorganic lithium-salt based dual-ion polymer electrolytes. Furthermore, good operability of the battery assembled with the electrolyte membrane in a wide temperature range was well demonstrated and significant performance at elevated temperatures was observed. The coulombic efficiency was found to be nearly 100% with the wide temperature range. Further enhancement of electrochemical performance can be envisaged through improvement of the compatibility between the electrolyte and the electrodes.

Experimental

Materials. Glutaric acid (Sigma-Aldrich), lithium aluminium hydride 1.0 M in diethyl ether (Sigma-Aldrich), anhydrous N, N-dimethylformamide (DMF) (Sigma-Aldrich), and acetonitrile (Tedia) were used as purchased. Hexamethyldisilazane (HMDS) (VWR international), 1, 2-dichloroethane (DCE) (Merck), methanol (Fisher) were distilled before use. All chemicals used were of reagent grade.

Preparation and characterization of $LiAl(OCH_3)_4$. $LiAl(OCH_3)_4$ was synthesized following the procedure proposed by Bakum.[41] Elemental analysis on $LiAl(OCH_3)_4$: calculated: C, 30.40; H, 7.65; Al, 17.07; Li, 4.39 %; found: C, 27.11; H, 5.96 Al, 17.86; Li, 4.73%. NMR spectra in DMSO-*d6*: ^{27}Al (in reference to 1M $Al(NO_3)_3$): 69.57 (br) ppm; ^{13}C: 48.54 ppm; ^{1}H: 3.18 ppm (s, 12H).

Preparation and characterization of silylated glutaric acid. The silylation was carried out under argon atmosphere by reacting glutaric acid 5.2848g (40 mmol) with 20.8 mL freshly distilled hexamethyldisilazane (HMDS) (100 mmol) as well as 0.5 mL trimethylsilyl chloride in anhydrous 1, 2-dicloroethane (DCE) at 100 ^{o}C for 6h. Upon cooling down to room temperature, DCE and excess HMDS were removed under a reduced pressure. ^{1}H NMR spectra in $CDCl_3$: 2.23 ppm (t, 4H), 1.75 ppm (m, 2H), 0.15 ppm (s, 18H).

Preparation and characterization of LiPGAA. The lithium poly(glutaric acid aluminate) (LiPGAA) was synthesized via polymerization between the silylated glutaric acid (40 mmol) and 3.1612g of $LiAl(OCH_3)_4$ (20 mmol) in an anhydrous DMF, stirring at 50 ^{o}C for 24 hrs and subsequently at 90 ^{o}C for 72 hrs. A white solid was first collected by filtration, then purified by Soxhlet extraction using acetonitrile as the solvent and finally by drying at 120 ^{o}C under a reduced pressure for 24hrs. Elemental analysis on $(C_{10}H_{12}AlLiO_8)_n$: calculated: C, 40.84; H, 4.11; Al, 9.17; Li, 2.36 %; found: C, 36.12; H, 4.54; Al, 10.53; Li, 2.44 %. CP-MAS NMR: ^{27}Al (in reference to 1 M $Al(NO_3)_3$) -5.72 ppm; ^{13}C (in reference to DMSO) 180.31 ppm, 36.07 ppm, 21.14 ppm.

The ^{1}H NMR and ^{13}C NMR spectra of $LiAl(OCH_3)_4$ and silylated glutaric acid were recorded on a Bruker AVANCE 500 spectrometer. The ^{13}C and the ^{27}Al magic angle spinning (MAS) NMR spectra of LiPGAA were recorded on a Bruker DRX-400 spectrometer, in reference to DMSO and 1M $Al(NO_3)_3$, respectively. The thermal stability of LiPGAA was investigated under nitrogen with a ramp of 10 ^{o}C min^{-1} from room temperature to 800 ^{o}C in the Thermo Gravimetric Analyzer (model TGA Q 50) of TA, Inst., USA. Powder X-Ray Diffraction (XRD) of the polymer was performed on a D5005 Bruker AXS diffractometer with Cu-Kα radiation (λ = 1.5410) in the scanning range between 1.4^{o}and 60^{o} at room temperature. The surface morphology of the compound and its composite membrane were imaged using JEOL JSM-6701F field emission scanning electron microscopy (FE-SEM). The samples were prepared by platinum-sputtering (30s, 20mA). Nitrogen sorption isotherms were measured up to 1 bar using a Micromeritics ASAP 2020 surface area and pore size analyzer. Before the measurements, the samples (~100 mg) were degassed under a reduced pressure (< 10^{-2} Pa) at 150 °C for 12 h. The UHP grade N_2 was used for the measurement. Oil-free vacuum pumps and oil-free pressure regulators were used to prevent contamination of the samples during the degassing process and isotherm measurement.

Electrolyte membrane preparation: PVDF-HFP and LiPGAA in a ratio of 3:1 (w/w) were added into a DMF solvent stirred at 80 ^{o}C to obtain a homogeneous dispersion. Subsequently, the dispersion was cast onto a teflon petri dish and kept in an oven at 80 ^{o}C for 12hrs. The obtained electrolyte membrane was dried further in a vacuum oven at 80 ^{o}C for 24hrs. Finally, the membrane was transferred into an argon-

filled glove box and placed in an EC: PC (V: V, 1:1) solution for soaking.

Electrode fabrication: Briefly, 80 wt.% of $LiFePO_4$, 10 wt.% of acetylene black, and 10 wt.% of poly(vinylidene fluoride) (PVDF) were mixed in NMP and magnetically stirred to form a slurry. The homogenous slurry was coated on an Al foil substrate and dried at 80 ^oC overnight under vacuum.

Electrochemical measurements: The ionic conductivity of the LiPGAA/PVdF-HFP blend membrane was measured using electrochemical impedance spectroscopy (Zahner, Zennium) over the frequency range of 1Hz-4MHz at an AC amplitude of 5 mV. The electrochemical stability measurement was conducted using a CHI workstation in the range from 2.5 V to 6.5 V at the rate of 1 mV/s. A lithium foil was employed as a counter and reference electrode. The lithium ion transference number was measured using the method proposed by Evans[40] by sandwiching the membrane between two lithium foil electrodes. After the initial resistance was measured, a potential of 10 mV was applied until a steady state was reached. Subsequently, the final resistance was measured by EIS. The galvanic charge-discharge experiments were carried out with the voltage in the range of 2.5-3.8V, using a multichannel battery testing instrument Arbin BT-2000.

Acknowledgements

The authors gratefully acknowledge support of this study by a start-up grant from NUS, a Tier 1 grant from Singapore Ministry of Education, a POC grant from National Research Foundation of Singapore, a Singapore DSTA grant and the grants from the National Natural Science Foundation of China (No. 21233006 and 21473164).

Notes and references

[a] *Department of Chemistry, National University of Singapore, 3 Science Drive 3, Singapore 117543. Email: Hansong Cheng: chghs2@gmail.com*

[b] *Sustainable Energy Laboratory, China University of Geosciences Wuhan, 388 Lumo RD, Wuhan 430074, China.*

Electronic Supplementary Information (ESI) available: [details of any supplementary information available should be included here]. See DOI: 10.1039/b000000x/

1. J. M. Tarascon and M. Armand, *Nature*, 2001, **414**, 359-367.
2. J. Maier, *Nat. Mater.*, 2005, **4**, 805-815.
3. P. G. Bruce, B. Scrosati and J.-M. Tarascon, *Angew. Chem. Int. Ed.*, 2008, **47**, 2930-2946.
4. B. Scrosati, *Nature*, 1995, **373**, 557-558.
5. J. B. Goodenough and K.-S. Park, *J. Am. Chem. Soc.*, 2013, **135**, 1167-1176.
6. K. Xu, *Chem. Rev.*, 2004, **104**, 4303-4418.
7. M. Doyle, T. F. Fuller and J. Newman, *Electrochim. Acta*, 1994, **39**, 2073-2081.
8. D. J. Bannister, G. R. Davies, I. M. Ward and J. E. McIntyre, *Polymer*, 1984, **25**, 1291-1296.
9. N. Kobayashi, M. Uchiyama and E. Tsuchida, *Solid State Ion.*, 1985, **17**, 307-311.
10. K. E. Thomas, S. E. Sloop, J. B. Kerr and J. Newman, *J. Power Sources*, 2000, **89**, 132-138.
11. B. K. Mandal, C. J. Walsh, T. Sooksimuang, S. J. Behroozi, S. Kim, Y. T. Kim, E. S. Smotkin, R. Filler and C. Castro, *Chem. Mat.*, 2000, **12**, 6.
12. X.-G. Sun and J. B. Kerr, *Macromolecules*, 2005, **39**, 362-372.
13. X.-G. Sun, C. L. Reeder and J. B. Kerr, *Macromolecules*, 2004, **37**, 2219-2227.
14. G. Cakmak, A. Verhoeven and M. Jansen, *J. Mater. Chem.*, 2009, **19**, 4310-4318.
15. R. Meziane, J.-P. Bonnet, M. Courty, K. Djellab and M. Armand, *Electrochim. Acta*, 2011, **57**, 14-19.
16. S. Feng, D. Shi, F. Liu, L. Zheng, J. Nie, W. Feng, X. Huang, M. Armand and Z. Zhou, *Electrochim. Acta*, 2013, **93**, 254-263.
17. S. Liang, U. H. Choi, W. Liu, J. Runt and R. H. Colby, *Chem. Mat.*, 2012, **24**, 2316-2323.
18. S. M. Renaud Bouchet, Rachid Meziane, Abdelmaula Aboulaich, Livie Lienafa, Jean-Pierre Bonnet, Trang N. T. Phan, Denis Bertin, Didier Gigmes, Didier Devaux, Renaud Denoyel & Michel Armand, *Nat. Mater.*, 2013, **12**, 6.
19. X. J. Wang, Z. H. Liu, C. J. Zhang, Q. S. Kong, J. H. Yao, P. X. Han, W. Jiang, H. X. Xu and G. L. Cui, *Electrochim. Acta*, 2013, **92**, 132-138.
20. Y. S. Zhu, X. J. Wang, Y. Y. Hou, X. W. Gao, L. L. Liu, Y. P. Wu and M. Shimizu, *Electrochim. Acta*, 2013, **87**, 113-118.
21. G. Xu, Y. Zhang, R. Rohan, W. Cai and H. Cheng, *Electrochim. Acta*, 2014, **139**, 264-269.
22. Y. Zhang, C. A. Lim, W. Cai, R. Rohan, G. Xu, Y. Sun and H. Cheng, *R. Soc. Chem. Adv.*, 2014, **4**, 43857-43864.
23. Y. Zhang, R. Rohan, W. Cai, G. Xu, Y. Sun, A. Lin and H. Cheng, *ACS Appl. Mater. interfaces*, 2014, **6**, 17534-17542.
24. Y. Zhang, R. Rohan, Y. Sun, W. Cai, G. Xu, A. Lin and H. Cheng, *R. Soc. Chem. Adv.*, 2014, **4**, 21163-21170.
25. T. J. Barbarich, S. M. Miller, O. P. Anderson and S. H. Strauss, *J. Mol. Catal. A: Chem.*, 1998, **128**, 289-331.
26. S. M. Ivanova, B. G. Nolan, Y. Kobayashi, S. M. Miller, O. P. Anderson and S. H. Strauss, *Chem. Eur. J.*, 2001, **7**, 503-510.
27. H. C. Brown and R. F. McFarlin, *J. Am. Chem. Soc.*, 1958, **80**, 5372-5376.
28. S. Tsujioka, B. G. Nolan, H. Takase, B. P. Fauber and S. H. Strauss, *J. Electrochem. Soc.*, 2004, **151**, A1418-A1423.
29. H. Tokuda, S.-i. Tabata, M. A. B. H. Susan, K. Hayamizu and M. Watanabe, *J. Phys. Chem. B*, 2004, **108**, 11995-12002.
30. H. Tokuda and M. Watanabe, *Electrochim. Acta*, 2003, **48**, 2085-2091.
31. K. Onishi, M. Matsumoto, Y. Nakacho and K. Shigehara, *Chem. Mat.*, 1996, **8**, 469-472.
32. T. Fujinami, A. Tokimune, M. A. Mehta, D. F. Shriver and G. C. Rawsky, *Chem. Mat.*, 1997, **9**, 2236-2239.
33. T. Aoki, A. Konno and T. Fujinami, *J. Electrochem. Soc.*, 2004, **151**, A887-A890.
34. G. D. Xu, Y. B. Sun, R. Rohan, Y. F. Zhang, W. W. Cai and H. S. Cheng, *J. Mater. Sci.*, 2014, **49**, 6111-6117.
35. Y. Zhang, Y. Sun, G. Xu, W. Cai, R. Rohan, A. Lin and H. Cheng, *Energy. Technol.*, 2014, **2**, 643-650.

36. R. Rohan, Y. Sun, W. Cai, K. Pareek, Y. Zhang, G. Xu and H. Cheng, *J. Mater. Chem. A.*, 2014, **2**, 2960-2967.
37. Y. Sun, R. Rohan, W. Cai, X. Wan, K. Pareek, A. Lin, Z. Yunfeng and H. Cheng, *Energy. Technol.*, 2014, **2**, 698-704.
38. O. E. Geiculescu, J. Yang, S. Zhou, G. Shafer, Y. Xie, J. Albright, S. E. Creager, W. T. Pennington and D. D. DesMarteau *J. Electrochem. Soc.*, 2004, **151**, A1363-A1368.
39. A. Ghosh, C. Wang and P. Kofinas, *J. Electrochem. Soc.*, 2010, **157**, A846-A849.
40. J. Evans, C. A. Vincent and P. G. Bruce, *Polymer*, 1987, **28**, 2324-2328.
41. N. Y. Turova, M. I. Karpovskaya, A. V. Novoselova and S. I. Bakum, *Inorg. Chim. Acta*, 1977, **21**, 157-161.

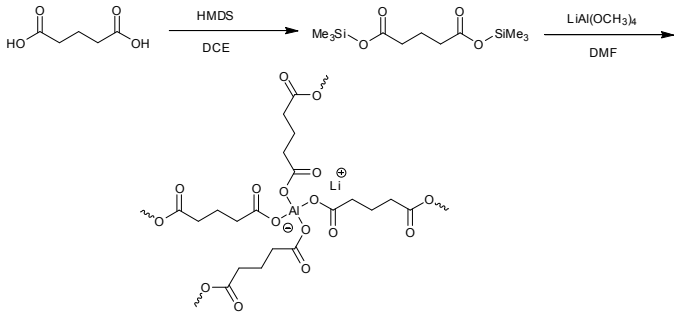

Scheme 1:Synthesis procedure of LiPGAA

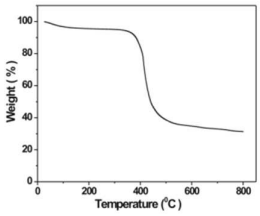

Fig. 1 TGA thermogram of LiPGAA (nitrogen, 10 °C/min, RT-800 °C)

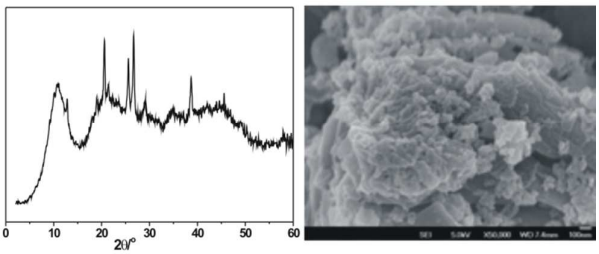

Fig. 2 PXRD (left) and FE-SEM image (right) of LiPGAA

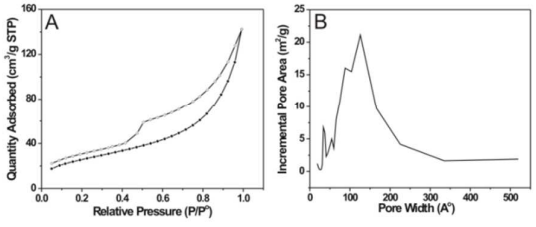

Fig. 3 Nitrogen sorption at 77K (A) and pore size distribution (B)

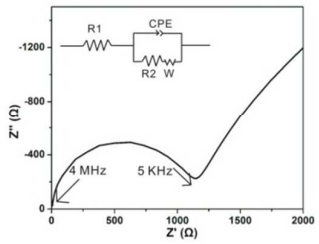

Fig. 4 The EIS plot of LiPGAA/PVDF-HFP composite membrane at room temperature with the corresponding equivalent circuit.

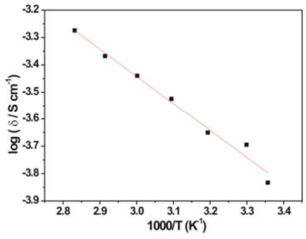

Fig. 5 Arrhenius plot of log(ionic conductivity) versus inverse absolute temperature

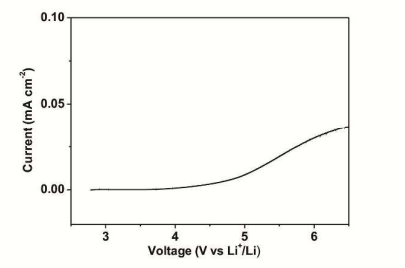

Fig. 6 The linear sweep voltammetry of the LiPGAA/PVDF-HFP composite membrane (scan rate 1 mV/s)

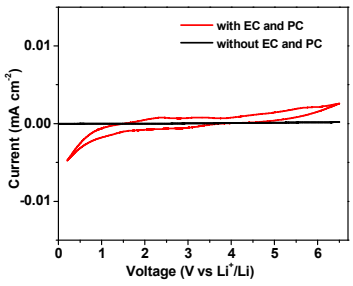

Fig. 7 The cyclic voltammetry of the LiPGAA/PVDF-HFP composite membrane with and without EC and PC

Table 1. The measured intial and steady-state currents, the initial and steady-state resistances of the passivation layers on the Li electrode and the Li-ion transference number

ΔV/ mV	I_0/μA	I_s/μA	R_0/ Ω	R_s/ Ω	t_{Li^+}
10	6.50	5.20	7.54	9.22	0.80

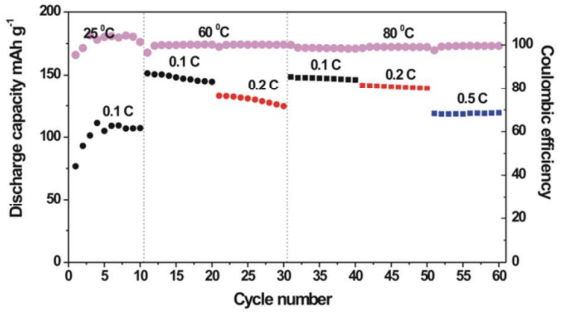

Fig. 8 The cycle performance of Li | LiPGAA/PVDF-HFP | $LiFePO_4$ battery in the temperature range of 25 °C to 80 °C and C/n rates

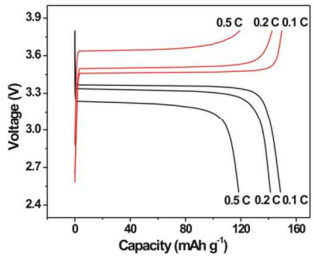

Fig. 9 The charge (red) /discharge (black) profiles at 80 °C and at C/n rates